

RESEARCH ARTICLE

Predictive Value of Asphericity in Pretherapeutic [^{111}In]DTPA-Octreotide SPECT/CT for Response to Peptide Receptor Radionuclide Therapy with [^{177}Lu]DOTATATE

Christoph Wetz,¹ I. Apostolova,¹ I. G. Steffen,² F. Hofheinz,³ C. Furth,² D. Kupitz,¹ J. Ruf,⁴ M. Venerito,⁵ S. Klose,⁶ Holger Amthauer²

¹Department of Radiology and Nuclear Medicine, University Hospital, Otto-von-Guericke University Magdeburg, Leipziger Strasse 44, 39120, Magdeburg, Germany

²Department of Nuclear Medicine, Charité-Universitätsmedizin Berlin, Augustenburger Platz 1, 13353, Berlin, Germany

³Institute of Radiopharmaceutical Cancer Research, PET Center, Helmholtz-Zentrum Dresden-Rossendorf, P.O. Box 51011901314, Dresden, Germany

⁴Department of Nuclear Medicine, University Hospital Freiburg, Hugstetter Strasse 55, 79106, Freiburg, Germany

⁵Department of Gastroenterology, Hepatology and Infectious Diseases, University Hospital, Otto-von-Guericke University Magdeburg, Leipziger Strasse 44, 39120, Magdeburg, Germany

⁶Department of Nephrology and Hypertension, Diabetology and Endocrinology, University Hospital, Otto-von-Guericke University Magdeburg, Leipziger Strasse 44, 39120, Magdeburg, Germany

Abstract

Purpose: The purpose of this study was to assess the value of the spatial heterogeneity of somatostatin receptor (SSR) volume, quantified as asphericity (ASP), and to predict response to peptide receptor radionuclide therapy (PRRT) in patients with metastatic gastroenteropancreatic neuroendocrine neoplasms (GEP-NEN).

Procedures: From June 2011 to May 2013, patients suffering from GEP-NEN who underwent pretherapeutic [^{111}In -DTPA⁰]octreotide scintigraphy (Octreoscan®) prior to [^{177}Lu -DOTA⁰-Tyr³]octreotate ([^{177}Lu]DOTATATE)-PRRT were enrolled in this retrospective evaluation. SSR expression in 20 NEN patients was qualitatively and quantitatively assessed using the Krenning score, the metastasis to liver uptake ratio (*M/L* ratio), and ASP at baseline. Response to PRRT was evaluated based on lesions, which were classified as responding lesions (RL) and non-responding lesions (NRL) after 4- and 12-month follow-ups. The values of the Krenning score, *M/L* ratio, and ASP for response prediction were compared by using the Mann-Whitney *U* test, Kruskal-Wallis test, and receiver operating characteristic (ROC) curves.

Results: Seventy-seven metastases (liver, *n* = 40; lymph node, *n* = 24; bone, *n* = 11; pancreas, *n* = 2) showed SSR expression. A higher ASP level was significantly associated with poorer response at both time points. ROC analyses revealed the highest area under the curve (AUC) for discrimination between RL and NRL for ASP after 4 months (AUC 0.97; *p* = 0.019) and after 12 months (AUC 0.96; *p* < 0.001), followed by the Krenning score (AUC 0.74; *p* = 0.082 and AUC 0.85; *p* < 0.001, respectively) and *M/L* ratio (AUC 0.77; *p* = 0.107 and AUC 0.82; *p* < 0.001). The optimal cutoff value for ASP was 5.12 % (sensitivity, 90 %; specificity, 93 %).

Conclusion: Asphericity of SSR-expressing lesions in pretherapeutic single-photon emission computed tomography with integrated computed tomography (SPECT/CT) is a promising parameter for predicting response to PRRT in gastroenteropancreatic neuroendocrine neoplasms.

Key words: Neuroendocrine neoplasm, Peptide receptor radionuclide therapy, [$^{111}\text{In-DTPA}^0$]octreotide scintigraphy, Asphericity

Introduction

Therapeutic options in patients with inoperable metastatic gastroenteropancreatic neuroendocrine neoplasms (GEP-NEN) are limited. The high-level expression of somatostatin receptors (SSR) 2 and 5 on the tumor cell surface in the majority of NEN provides the basis not only for sensitive functional imaging with radioisotope-labeled somatostatin analogues but also for a tumor-targeted radiotherapy with beta emitters [1].

Commonly, “cold” somatostatin analogues, such as octreotide long-acting repeatable, are the first-line antiproliferative therapy in patients with SSR-positive NEN. The combination with everolimus can intensify the antitumor efficacy of the somatostatin analogues and improve progression-free survival (PFS) [2]. Very promising results have been published concerning patients undergoing peptide receptor radionuclide therapy (PRRT) with [$^{177}\text{Lu-DOTA}^0\text{-Tyr}^3$]octreotate ([^{177}Lu]DOTATATE) after disease progression under octreotide [3]. NETTER-1, the first prospective randomized study in patients with progressive metastatic midgut NEN, showed the superiority of [^{177}Lu]DOTATATE-PRRT to octreotide regarding PFS [4].

SSR expression and density are reported to be variable in metastatic lesions of NEN, irrespective of tumor differentiation and grading [5]. Several studies have shown that NEN patients with higher lesional SSR expression exhibit an improved therapy response compared with those with low SSR uptake [6]. The Krenning score, a well-established qualitative surrogate parameter [3, 7], and the metastases to liver ratio (*M/L* ratio), a scanner-independent quantitative measure [8], are the most common approaches for prediction of response to therapy using PRRT based on assessment of receptor expression. However, both parameters only focus on the extent of receptor expression, while NEN biological behavior and response to therapy are also defined by other factors such as clinical and pathological features, size, and proliferation index [9]. Therefore, imaging parameters, which reflect further features of tumor behavior, might contribute to more accurate characterization of NEN metastatic lesions in order to stratify patients, to ensure individualized treatment schedules, and to minimize side effects.

In particular, tumor heterogeneity was suggested to correspond to cellular proliferation, necrosis, angiogenesis, and hypoxia in metabolic 2-deoxy-2-[^{18}F]fluoro-D-glucose ([^{18}F]FDG) positron emission tomography (PET)/x-ray computed tomography (CT) studies [10, 11], indicating

aggressive tumor behavior [12]. Corresponding observations have also been made for the heterogeneity of SSR expression in metastasized thyroid carcinoma prior to PRRT [13], explained by the fact that a homogeneous and uniform SSR expression raises the possibility of a consecutively uniformly high tumoral irradiation dose. In addition, loss of cellular receptor expression might be the result of further tumor dedifferentiation, further aggravating prognosis. However, as reliable and complete assessment of the tumor SSR uptake merely based on biopsy may not adequately represent the *in vivo* intratumoral functional diversity, imaging-based heterogeneity by indices such as asphericity (ASP) might help resolve this problem.

A cost-effective and widely available method for planning PRRT is tumor dosimetry by using [$^{111}\text{In-DTPA}^0$]octreotide ([^{111}In]octreotide, Octreoscan®) scintigraphy [14]. Octreotide single-photon emission tomography (SPECT) with integrated computed tomography (CT) as a hybrid imaging modality is highlighted as a clinically established imaging tool for evaluation of NEN [15, 16]. In head, neck, and lung cancer, the assessment of ASP, *i.e.*, the quantification of a lesion’s spatial heterogeneity, has emerged as a very promising parameter in terms of predicting response to therapy by assessment of metabolic tumor volumes in [^{18}F]FDG-PET/CT [17–20]. Analogous to the approaches in oncological [^{18}F]FDG-PET, the aim of our study is to test the value of ASP for response prediction in somatostatin-positive lesions using octreotide SPECT. Established parameters such as Krenning score and *M/L* ratio were used for comparison. To our knowledge, qualitative and quantitative analyses of the spatial heterogeneity of receptor density in NEN metastases have not yet been reported.

Methods

Patients

Twenty patients (f, $n = 6$; m, $n = 14$; mean age, 72.6 ± 9.5 years, range, 54 to 87 years) with histologically confirmed metastatic NEN who underwent PRRT during the period from June 2011 to May 2013 were retrospectively enrolled.

The inclusion criteria were as follows: (1) octreotide SPECT/CT for evaluation of SSR positivity prior to PRRT, (2) patients who consequently received at least two cycles of PRRT, (3) follow-up of ≥ 12 months, and (4) available SPECT/CT data sets for analysis.

All patients had progressive metastasized NEN disease, and surgical intervention was not a treatment option. All NENs were low or intermediate grade (G₁ or G₂), and an interdisciplinary tumor board decision for PRRT was available. All treated patients had SSR-positive lesions determined by SPECT/CT with [¹¹¹In]octreotide prior to therapy.

Patients obtained two to four cycles (median, 3; IQR, 3–3.25; range, 2–4) of PRRT with an average dose of 200 mCi (7.450 GBq) [¹⁷⁷Lu]DOTATATE per cycle. Patients underwent first response assessment after two cycles of [¹⁷⁷Lu]DOTATATE, after an interval of 8 weeks. If patients showed disease relapse, therapy was discontinued immediately. In case of response to therapy, patients obtained third, and up to fourth, cycles of [¹⁷⁷Lu]DOTATATE-PRRT. The therapy decision and the number of therapy cycles were determined in interdisciplinary meetings for each individual patient on the basis of the first restaging after 4 months. The number of cycles is illustrated in Table 1.

[¹¹¹In]Octreotide (Octreoscan®)

Octreotide is a synthetic somatostatin analogue, labeled with In-111 ($T_{1/2} = 2.81$ days) [21]. It specifically binds to SSR and is available as a commercial kit (Octreoscan®, Mallinckrodt Radiopharmaceuticals, Dublin, Ireland, UK) and was labeled according to the manufacturer's instructions.

Imaging Techniques

Imaging with [¹¹¹In]octreotide was performed in accordance with current guidelines [22, 23]. Planar imaging was performed with a dual head SPECT/CT device (Discovery NM/CT670, GE, Haifa, Israel) according to standard protocols. Additionally, SPECT with low-dose CT of the thorax and abdomen was performed at 24 and 48 h post-injection (p.i.) (SPECT-ldCT24 and SPECT-ldCT48)

using MEGP collimators and energy window settings (60 frames; 40 s per frame [step and shoot]; 6° angles; matrix, 128 × 128; field of view, 540 cm × 400 cm; rough overlap, 4 cm; $E_{\text{peak}} = 208 \text{ keV} \pm 10 \%$).

SPECT data was reconstructed iteratively (OSEM 2 iterations, 10 subsets) with CT-based correction for attenuation using the low-dose CT (40 mA, 120 kV, 3.75 mm slice thickness). Imaging data were evaluated using a dedicated workstation (Xeleris-Workstation, GE Healthcare, Waukesha, USA) at standard clinical settings.

A diagnostic contrast-enhanced CT scan (dCT24) was performed at 24 h p.i. using a multiphase protocol consisting of an arterial (delay, 25 s) and portal-venous phase (delay, 45 s) for the upper abdomen and a delayed venous phase (delay, 70 s) for thoracoabdominopelvic imaging (mAs, 50–300, as modified by body region and automatic dose modulation [AutomA®]; voltage, 120 kV; collimation, 16 × 1.25 mm; pitch, 1.375; slice thickness, 16 × 1.25 mm) after weight-dependent administration of 70–100 ml of intravenous contrast medium (Imeron 300, Bracco Imaging Deutschland GmbH, Konstanz, Germany).

MRI of the liver was performed according to a standard protocol, which has been published elsewhere [24].

Image Analysis

CT (contrast-enhanced, CE-CT) and MRI (contrast-enhanced, CE-MRI) were used for assessment of morphological changes by quantifying the lesion's diameter at an initial point prior to therapy (mean, 3 weeks; range, 1–5 weeks). Baseline CT/MRI data were obtained for treatment planning and [¹¹¹In]octreotide was assessed for evaluation of SSR positivity prior to PRRT treatment (time to PRRT: mean, 4 weeks, range, 2–7 weeks). All patients obtained CE-CT scan as follow-up examination but only 16 obtained also MRI.

Accounting for study quality and to ensure inpatient comparability between baseline and follow-up studies, CE-CT

Table 1. Patient data and overview of RLs and NRLs

	Sex	Age	Primary localization	Grading	Cycles of PRRT	Liver MT	Lymph node MT	Bone MT	Pancreatic MT
1	m	79	GI-NEN	G2	4	2 RL			
2	m	54	GI-NEN	G2	3	2 RL	2 RL		
3	m	71	GI-NEN	G2	3	2 NRL	1 NRL		
4	m	62	CUP-NEN	G1	3	2 RL	2 RL	1 RL	
5	f	67	P-NEN	G2	2	1 RL/ 1 NRL	2 NRL		1 NRL
6	m	55	GI-NEN	G1	3	2 RL			
7	f	79	GI-NEN	G2	2	2 NRL	2 NRL	1 RL	
8	f	71	GI-NEN	G2	3	2 RL			
9	m	79	GI-NEN	G2	3	2 RL	2 RL		
10	f	67	CUP-NEN	G1	3	2 NRL	1 RL / 1 NRL	1 RL	
11	m	84	GI-NEN	G2	3	2 RL			
12	f	66	GI-NEN	G2	2	2 NRL			
13	f	64	CUP-NEN	G2	4	2 RL	2 RL	1 RL	
14	m	80	GI-NEN	G1	3	2 RL	2 RL		
15	m	71	GI-NEN	G1	3	2 NRL		2 NRL	
16	m	76	GI-NEN	G1	2	2 RL	2 RL	1 RL	
17	m	86	GI-NEN	G2	4	2 RL	2 RL		
18	m	87	GI-NEN	G1	3	2 RL	1 RL	2 RL	
19	m	78	P-NEN	G2	4	2 RL	2 RL		1 RL
20	m	76	CUP-NEN	G1	4	2 RL		2 RL	

Number of cycles of [¹⁷⁷Lu]DOTATATE-PRRT peptide receptor radionuclide therapy

RL responding lesions, NRL non-responding lesions, m male, f female, CUP-NEN neuroendocrine neoplasm of unknown primary, P-NEN pancreatic neuroendocrine neoplasm, GI-NEN gastrointestinal neuroendocrine neoplasm, MT metastases

was used as the main modality for follow-up assessment. All patients underwent follow-up CE-CT at 4, 8, and 12 months after the first cycle of [¹⁷⁷Lu]DOTATATE-PRRT. In cases in which MRI was available, it was used for morphological correlation and further characterization of liver lesions. MRI was performed 4 and 12 months after the first therapy cycle.

The lesions were assessed quantitatively with respect to changes in diameter at each time point and were classified according to the new response evaluation criteria in solid tumors (RECIST 1.1) as progressive disease (PD), stable disease (SD), partial response (PR), and complete remission (CR) [25]. The lesion diameter obtained at the initial staging was compared to the lesion diameter at the 12-month follow-up and categorized as responding lesion (RL [SD, PR, CR], $n = 57$) or non-responding lesion (NRL [PD], $n = 20$). Additionally, following the RECIST 1.1 guidelines, only lesions in CE-CT or CE-MRI with a short axis of ≥ 10 mm (liver, pancreas metastases) and ≥ 15 mm (lymph nodes, bone lesions) were considered measurable and assessable as target lesions. Lymph nodes < 10 mm diameter were assumed to be normal. Two lesions per organ and no more than five lesions per patient were included [25]. In the case of more than two metastases per organ, we included two “representative” lesions with the highest SSR uptake on visual assessment. Four months and 12 months after the first cycle [¹⁷⁷Lu]DOTATATE-PRRT, lesions were classified into two subgroups: RLs if the short axis did not change or was decreased or NRLs if the short axis increased by at least 20 % and showed an absolute increase of at least 5 mm in diameter. According to RECIST 1.1, a 5-mm absolute increase in lesion diameter is required to document progress in order to account for the limited spatial resolution of CT and MRI. Thus, a small increase (< 5 mm) of the target lesion was not interpreted as progress.

Therapy was discontinued after two cycles of [¹⁷⁷Lu]DOTATATE-PRRT in four patients because of tumor progression. Therefore, to achieve a homogeneous assessment of the whole patient group, the first evaluation was performed at 4 months. Considering the rather slow tumor growth in GEP-NEN, a second assessment was performed after 12 months.

The Krenning score was used to qualitatively describe avidity of lesions to the administered radiopharmaceutical (i.e., no uptake: 0; faint uptake: 1; clear uptake in the lesion but less than in the liver: 2; uptake greater in the lesion than in the liver: 3; uptake much greater in the lesion than in the liver: 4) [3]. The Krenning score was assessed using planar imaging.

The M/L ratio was calculated as the maximum signal intensity (SI) of the lesion divided by the standard deviation of the background activity in normal liver tissue. The background value was determined from the standard deviation of a circular region of interest (ROI) placed in the unaffected liver tissue [8].

ASP is a quantitative approach to assess the spatial heterogeneity (asphericity) of SSR functional volume in NEN lesions. We hypothesize that an apparently inhomogeneous cell surface expression of SSR leads to increasing tumor asphericity and, thus, increases the ratio of surface area and volume of the functionally active SSR-positive part of the tumor lesion.

To assess the functionally active part of the neuroendocrine metastases, a standardized volume of interest (VOI) was drawn around each lesion. VOI definition and analysis were performed to compute ASP using ROVER version 2.1.20 (ABX, Radeberg, Germany). Pretherapeutic [¹¹¹In]octreotide SPECT was used for assessment of ASP.

SSR-positive lesions were delineated by an automatic algorithm based on adaptive thresholding accounting for the local background [26, 27]. The result of the automatic delineation was inspected visually, and if metastases overlapped or other non-tumor tissue was included in the VOI, the volume delineation was corrected manually ($n = 30$, 39 %). The ASP of neuroendocrine metastases is given by

$$\text{ASP} = \sqrt[3]{H-1} \text{ with } H = \frac{1}{36\pi} \frac{S^3}{V^2}$$

where S is the mean surface area and V is the mean volume. It can be simplified as follows: for non-spherical shapes, ASP delivers a quantitative degree of deviation from a “perfect” sphere, resulting in $\text{ASP} > 0$. Additional detailed method description is given in [10, 17–20].

The lesion diameter was measured using CE-CT and CE-MRI according to the RECIST 1.1 criteria manually using INFINITT software (INFINITT Healthcare Co., Ltd., 12F Daerung Post Tower III, 182-4 Guro-dong, Guro-gu, Seoul, 152-050, South Korea).

In all patients, diagnostic CE-CT and CE-MRI scans were performed prior to somatostatin receptor scintigraphy (SRS).

Statistical Analysis

Data analyses were accomplished by using SPSS 22 (IBM Corporation, Armonk, NY, USA). According to histograms and quantile-quantile plots, non-parametric distribution of data was assumed. Values were expressed as median, interquartile range (IQR, 25th percentile–75th percentile), and range (minimum–maximum) and depicted as boxplots. The Krenning score, M/L ratio, and ASP for response prediction were compared using the Kruskal-Wallis test and Mann-Whitney U test for unpaired data as well as area under the curves (AUC) of receiver operating characteristic (ROC) curves. The optimal cutoff values were assessed using Youden’s index, separately for the 4- and 12-month assessments. The three surrogate parameters were binarized using optimal ROC cutoff values, and sensitivity and specificity were calculated. All tests were two-sided, and statistical significance was considered at $P < 0.05$ and high significance at $P < 0.001$.

Results

Seventy-seven metastatic NEN lesions (liver, $n = 40$; lymph node, $n = 24$; bone, $n = 11$; pancreatic, $n = 2$) were observed. There were no significant differences in the maximum diameters of RLs and NRLs during initial pre-therapy assessment (RL, 19.7 mm; IQR, 13.4–29.5 vs. NRL, 16.2 mm; IQR, 12.9–31.2; $p > 0.05$). The mean functional volume was computed by using software with background-corrected threshold detection (ROVER) and was 9.3 ml for all lesions at baseline (IQR, 6.7–23.9 ml; range, 2.4–213.2 ml). There was also no significant difference in functional volume between RLs and NRLs prior to [¹⁷⁷Lu]DOTATATE-PRRT ($p > 0.05$).

Lesion Response

In the RLs, the median NEN lesion size (max. diameter) decreased to 17.1 mm (IQR, 13.1–29.0; range, 1.0–62.0) at the 4-month follow-up. The decrease of the lesion size of RLs after 4 months was significant ($p < 0.01$). The mean NEN lesion size in NRLs increased to 20.6 mm (IQR, 8.1–76.0; range, 15.7–34.5) after treatment. There was a highly significant difference in the diameter of RLs and NRLs after two cycles of [^{177}Lu]DOTATATE-PRRT (17.1 mm; IQR, 13.1–29.0 vs. 20.6 mm; IQR, 8.1–76.0; $p < 0.001$).

After 12 months, the mean NEN lesion size in RLs decreased to 13.4 mm (IQR, 9.0–25.2; range, 0.0–61.0). In the NRLs, the mean lesion size was 25.1 mm (IQR, 18.6–47.0; range, 11.0–80.7) after treatment. There was a highly significant difference in the diameter of RLs and NRLs compared at initial measurement and after treatment (13.4 mm; IQR, 9.0–25.2 vs. 25.1 mm; IQR, 18.6–47.0; $p < 0.001$).

Fig. 1 presents a typical example of an RL, and Fig. 2 shows a representative case of an NRL. Table 1 shows detailed patient and lesion characteristics.

Response According to RECIST 1.1

After 12 months, 57 (74 %) of the observed metastases showed therapy response (RL). SD was achieved in 27

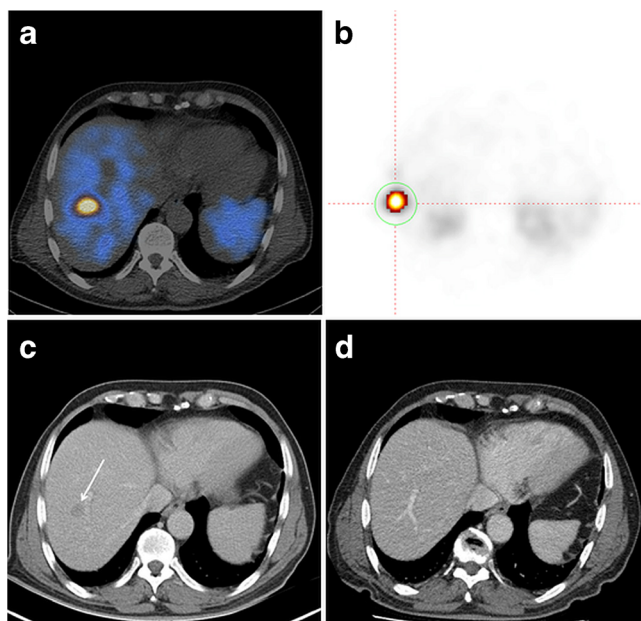


Fig. 1 Representative responding lesion (RL). **a** Representative example of one responding lesion, 4.2 ml, and an ASP value of 1.4 %; **b** ASP measurement using the ROVER software is illustrated in red-white. **c** An 80-year-old man with GEP-NEN and liver metastases prior to therapy with [^{177}Lu]DOTATATE-PRRT showing an exemplary lesion with a maximum diameter of 2.0 cm on the CE-CT. **d** After four cycles of PRRT, complete response was achieved. CT images pre- and post-therapy were matched manually according to anatomical landmarks.

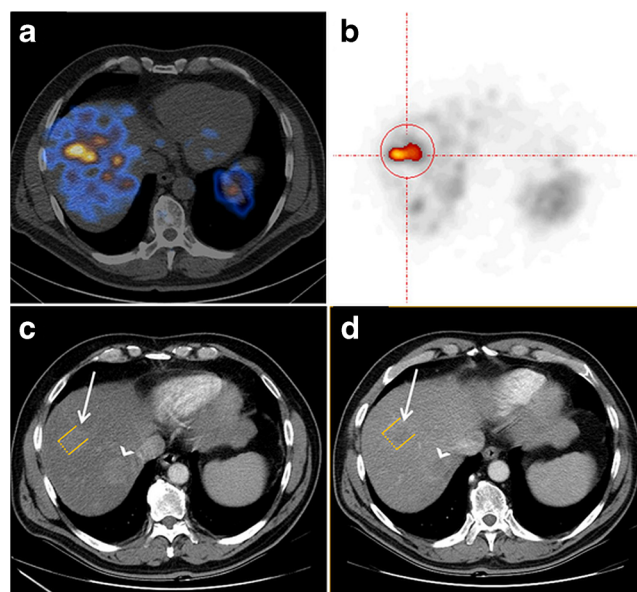


Fig. 2 Representative non-responding lesion (NRL). Representative example of one non-responding lesion. A 64-year-old man with GEP-NEN and liver metastases undergoing three cycles of [^{177}Lu]DOTATATE-PRRT. An exemplary lesion is shown with a maximum diameter of 2.3 cm (vol. 5.8 ml) on **a** OctreoScan and **c** CE-CT prior to therapy. **b** ASP measurements revealed an ASP value of 13.2 %, illustrated in red-white. **c** The tumor measurement is displayed by a white arrow and maximum diameter is highlighted in orange. **d** After treatment, the maximum diameter of the tumor lesion increased to 3.2 cm with a tumor volume of 15.7 ml. Triangular arrowheads point at a secondary finding—an additional hepatic metastasis with increasing diameter.

(35 %) of all lesions. Reduction in size according to PR was seen in 14 (18 %) metastases, whereas CR was observed in 21 % of cases ($n = 16$). However, an increase in diameter was seen in 20 (26 %) metastases (PD).

Per-patient analyses revealed PR in 11 patients (55 %). In 15 % of the study group ($n = 3$), mixed response was shown (some of the treated metastases showed regression in size, others showed stable diameter). Progressive disease (PD), determined by an increasing lesion diameter, was observed in 30 % ($n = 6$) of all patients. Detailed lesion description is reported in Table 2.

Association of ASP, M/L Ratio, and Krenning Score

Higher ASP was significantly associated with poorer response: PD, 9.8 (IQR, 6.1–15.4; range, 2.2–18.0); SD, 2.7 (IQR, 1.6–4.1; range, 0.0–7.3); PR, 1.3 (IQR, 0.4–2.4; range, 0.0–6.0); and CR, 0.5 (IQR, 0.0–1.1; range, 0.0–2.0; Kruskal-Wallis, $p < 0.001$). The median ASP in the RLs prior to PRRT was 1.4 % (IQR, 0.5–3.3; range, 0.0–7.3) and significantly lower (Wilcoxon, $p < 0.001$) compared to that of NRLs (PD).

Table 2. PRRT—response to therapy

MDA criteria		Liver MT	Lymph node MT	Bone MT	Pancreas MT	Sum	Percent
RL		29	18	9	1	57	74 %
	CR	9	5	2		16	21 %
	PR	6	4	3		14	18 %
	SD	14	6	2	1	27	35 %
NRL	PD	11	6	2	1	20	26 %
Total		40	24	11	2	77	100 %

Metastases in systematic overview: the impact on *RL* and *NRL* after [¹⁷⁷Lu]DOTATATE-PRRT (peptide receptor radionuclide therapy)
RL responding lesions, *NRL* non-responding lesions, *MDA criteria* minimal disease activity criteria, *MT* metastases

The Krenning score was significantly associated with response as well, and higher score values showed a better

response: PD, 2 (IQR, 1.0–2.0; range, 1.0–3.0); SD, 2 (IQR, 2.0–3.0, range; 2.0–3.0); PR, 3 (IQR, 3.0–3.3; range,

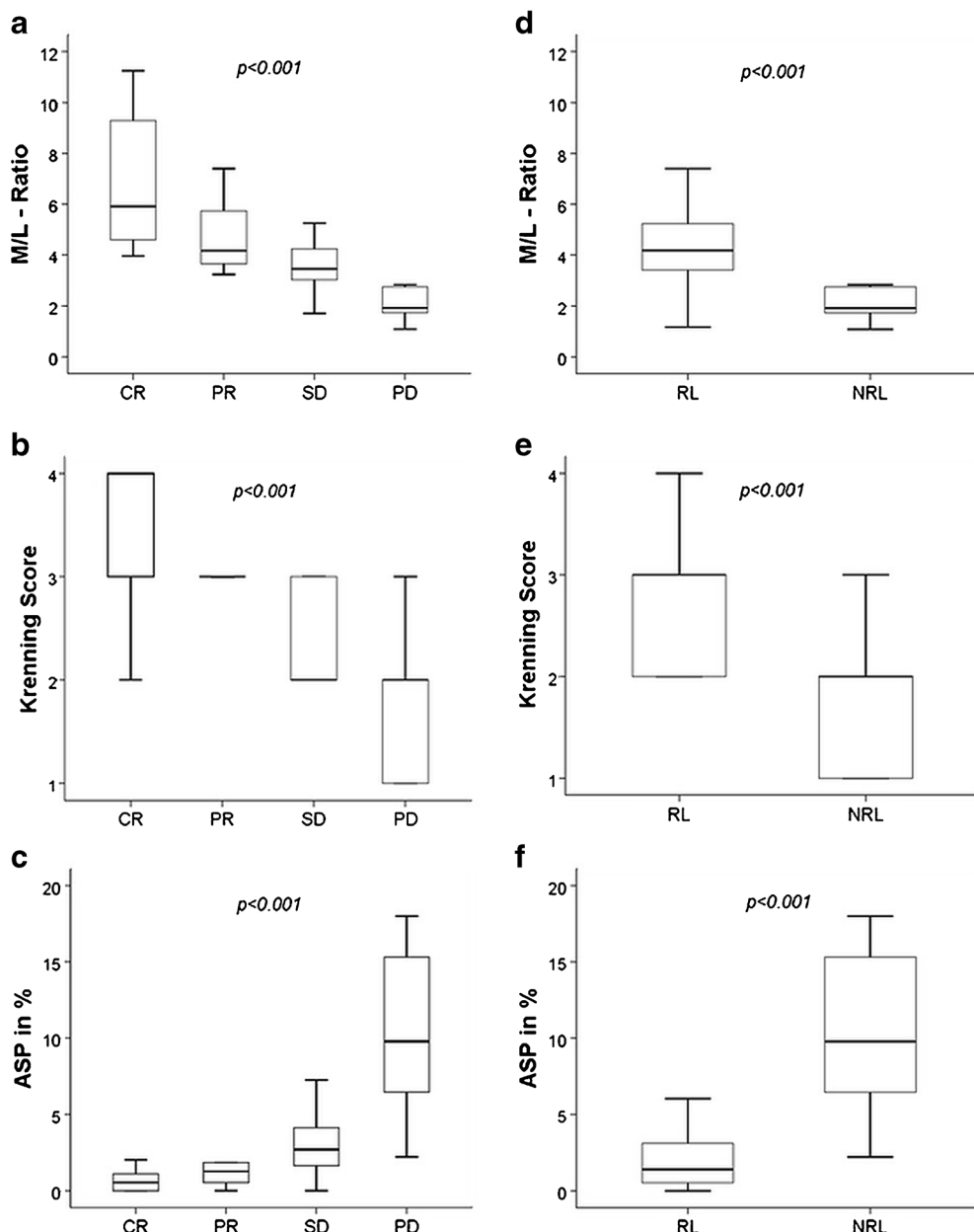


Fig. 3 Box plot analysis of ASP, Krenning score, and *M/L* ratio after 12-month follow-up **a–c** according to the four response groups (CR, PR, SD, PD; Kruskal-Wallis, $p < 0.001$) and **d–f** in responding lesions (RL) vs. non-responding lesions (NRL; Wilcoxon, $p < 0.001$).

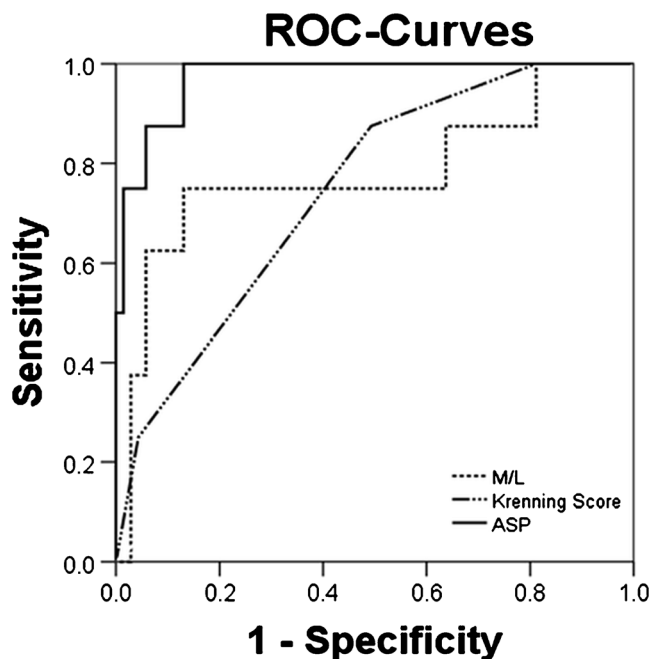


Fig. 4 ROC curve comparison after 4 months. After 4 months and two cycles of [^{177}Lu]DOTATATE-PRRT, the *M/L* ratio (metastases to the liver) presented a higher AUC than the Krenning score (Krenning score AUC = 0.75, $p < 0.024$; *M/L* ratio AUC = 0.77, $p < 0.011$). The ROC of ASP showed highly significant results (AUC = 0.97, $p < 0.001$).

2.0–4.0); and CR, 4 (IQR, 3.0–4.0; range, 2.0–4.0; $p < 0.001$). The Krenning score of RLs (3; IQR, 2–3; range, 2–4) was significantly higher ($p < 0.01$) compared to that of NRLs (PD).

Higher *M/L* ratios were significantly associated with better response: PD, 1.9 (IQR, 1.7–2.8; range, 1.1–7.1); SD, 3.5 (IQR, 3.0–4.3; range, 1.2–5.3); PR, 4.2 (IQR, 3.6–5.7; range, 3.2–7.4); and CR, 5.9 (IQR, 4.6–9.3; range, 4.0–11.2; $p < 0.001$). The median *M/L* ratio for RLs was 4.2 (IQR, 3.4–5.2; range, 1.2–11.2) and significantly higher ($p < 0.001$) compared to that of NRLs (Fig. 3).

After 4 months and two cycles of [^{177}Lu]DOTATATE-PRRT, interim ROC analyses showed the highest AUC for ASP (AUC 0.97, $p < 0.019$) followed by the Krenning score (AUC 0.74, $p < 0.082$) and *M/L* ratio (AUC 0.77, $p < 0.107$). Calculation of Youden's index at 4 months revealed an optimal cutoff for ASP at 6.59 % (sensitivity and specificity, 87.5 and 87.0 %), for Krenning score at 3 (sensitivity and specificity, 87.5 and 51.0 %), and for *M/L* ratio at 3.12 (sensitivity and specificity, 75.4 and 73.8 %), respectively (Fig. 4).

After 12 months, ROC analyses also revealed the highest AUC for ASP to differentiate between RL and NRL (AUC 0.96, $p < 0.001$), followed by the Krenning score (AUC 0.85, $p < 0.001$) and *M/L* ratio (AUC 0.82, $p < 0.001$). Calculation of Youden's index revealed an optimal cutoff to

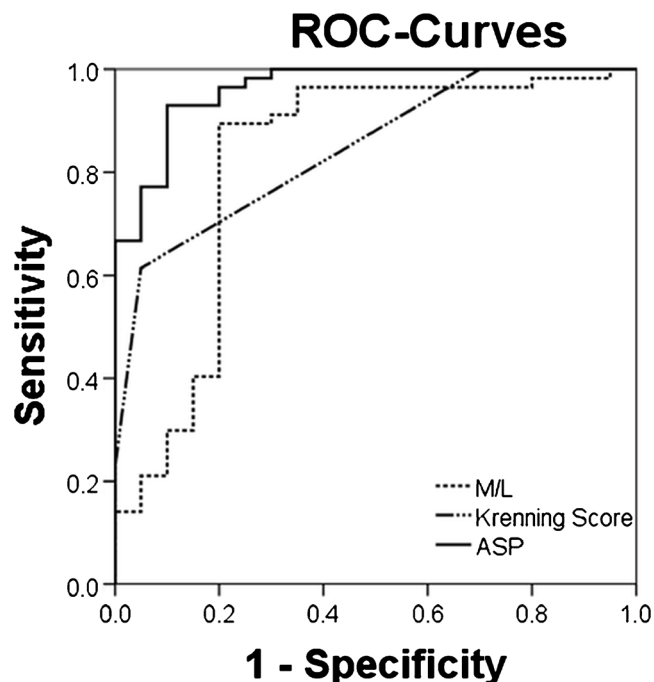


Fig. 5 ROC curve comparison after 12 months. After 12 months, ASP showed the highest AUC of 0.96, followed by the Krenning score and *M/L* ratio (Krenning score AUC = 0.85, *M/L* ratio AUC = 0.82).

discriminate between responding and non-responding lesions for ASP at 5.12 % (sensitivity and specificity, 90.0 and 93.0 %, respectively), for the Krenning score at 3 (sensitivity and specificity, 58.1 and 95.4 %), and for the *M/L* ratio at 2.90 (sensitivity and specificity, 89.5 and 80.0 %; Fig. 5).

Discussion

This study aimed for quantitative characterization of the shape heterogeneity of SSR-positive NEN lesions as a parameter for predicting response to PRRT. To this end, we were able to demonstrate that the spatial SSR distribution in NEN metastases was predictive of response to PRRT.

[^{111}In]octreotide, a somatostatin-derived radiolabeled peptide, is used as a method of choice for *in vivo* scintigraphy of SSR-positive NENs before PRRT [28]. It binds primarily to SSR₂ (IC₅₀ = 22 ± 3.6 nM) and, to a lesser extent, SSR₅ (IC₅₀ = 237 ± 52 nM), subclass receptors. [^{111}In]octreotide is considered a predictive surrogate regarding [^{177}Lu]DOTATATE binding despite the tenfold higher affinity of [^{177}Lu -DOTA⁰,Tyr³]octreotate to SSR₂ (IC₅₀ = 1.5 ± 0.4 nM) and a similar affinity to SSR₅ (IC₅₀ = 547 ± 160 nM) [29, 30]. In addition, in modern clinical practice, the octreotide SPECT is coregistered with low-dose CT. This leads to an increase of specificity due to better anatomical mapping [28].

In addition to somatostatin expression, there are important factors to be considered for an effective therapy, such as size, lesion heterogeneity, and location [31]. The Krenning score was one of the first approaches for visual assessment and stratification of the accumulating amount of the radioligand as a surrogate for SSR₂ receptor expression. Krenning *et al.* found [¹¹¹In]octreotide scintigraphy to be a reliable parameter to predict response to PRRT [3]. The *M/L* ratio as a scanner-independent tool provides a semi-quantitative estimation of receptor status and was also found to be useful in predicting therapy response to PRRT [8]. In this study, parameters such as the Krenning score, *M/L* ratio, and ASP of [¹¹¹In]octreotide scintigraphy were compared and correlated with each other regarding the patient's outcome after receiving [¹⁷⁷Lu]DOTATATE-PRRT. Although the Krenning score is known to be a pan-lesional surrogate parameter, it is, in tandem with the *M/L* ratio, mainly focused on small heterogeneous regions with maximal tumor receptor expression, rather than whole tumor uptake and shape. It has been shown that further biological parameters, such as grade of differentiation, are associated with tumor heterogeneity, size, and aggressiveness [9, 31]. ASP provides the opportunity to assess quantitatively the lesion's heterogeneity in SRS, which might depict some features associated with tumor behavior.

Even as early as after two cycles of [¹⁷⁷Lu]DOTATATE-PRRT at interim staging, ASP emerged as the most significant surrogate parameter (sensitivity and specificity, 88 and 87 %) in contrast to the Krenning score and *M/L* ratio. Thus, ASP can be used to distinguish between responding and non-responding patients. Since four cycles of [¹⁷⁷Lu]DOTATATE-PRRT is a time-consuming therapy, non-responders may benefit from an early therapy switch.

Considering the rather slow tumor growth in GEP-NEN, a second analysis was performed based on the follow-up studies after 12 months in order to classify lesions into four response groups (CR, PR, SD, PD) and as RLs vs. NRLs. Restaging 12 months after completion of therapy is considered a standard in GEP-NEN.

We included the Krenning score in the analysis as an established visual parameter in terms of prediction of response to PRRT. At a cutoff of 3, the sensitivity and specificity were 58 and 95 %, respectively. Krenning *et al.* and Srirajaskanthan *et al.* [3, 32] assumed a cutoff of 2 as a highly predictive tool in achieving response. We also determined the ratio between the maximum grayscale intensity of NEN metastases relative to the liver background uptake (*M/L* ratio) with a cutoff of 2.90 (sensitivity and specificity, 90 and 80 %). Kratochwil *et al.* [8] recommended, in a [⁶⁸Ga-DOTA⁰-Phe¹-Tyr³]octreotide (DOTATOC)-PET/CT study, a scanner-independent cutoff of 2.2 (sensitivity and specificity, 95 and 20 %). However, this parameter showed rather low specificity. Using the recommended cutoff in our patient sample, a sensitivity of 96 % and specificity of 45 % were achieved.

ASP outperformed the other established measures for predicting RL of NEN metastases (sensitivity and specificity, 90 and 93 %, at a cutoff of 5.12 %).

In our patient group, the Krenning score and *M/L* ratio showed limitations, especially in liver metastases with high heterogeneous tumor receptor expression. These results suggest that ASP delivers useful additional prognostic information in terms of response to PRRT. Furthermore, increasing tumor heterogeneity might be a potential paradigm for irregular (partly decreased) SSR expression, which is accompanied by dedifferentiation. The extent of SSR expression directly affects the success of [¹⁷⁷Lu]DOTATATE-PRRT. Accordingly, ASP depicted more accurately the biological tumor aggressiveness.

The importance of tumor heterogeneity assessment has also been recently shown by Lapa *et al.* [13], who evaluated the prognostic value of tumor heterogeneity assessed by [⁶⁸Ga-DOTA⁰-Tyr³]octreotate (DOTATATE) PET/CT or [⁶⁸Ga]-DOTATOC-PET/CT in patients with iodine-refractory differentiated and advanced medullary thyroid cancer prior to PRRT, albeit parameters such as entropy instead of ASP were determined.

The Krenning score is a purely subjective visual score and thus introduces a strong limitation in reproducibility of results. Contrary to the Krenning score, intra- and inter-observer variability might be diminished by the semi-automatic algorithm of VOI definition and subsequent VOI delineation. This, however, has not been examined in the current work. The application of ASP is limited in lesions smaller than 2.5 ml [17], *e.g.*, lymph nodes. Considering a limited spatial resolution of SPECT/CT imaging—especially with [¹¹¹In]octreotide—small lesions are more likely to appear with a symmetrical sphere shape. This might adulterate the results in smaller lesions. However, due to the small number of lesions with a volume <2.5 ml in the current analysis (3 lesions out of 77 metastatic lesions in total), we believe that this fraction of lesions does not have an essential impact on the main results. Further limitations may arise from the retrospective single-center setting of the study and the limited sample size. A prospective validation is required in a larger setting.

Conclusion

Our results indicate that asphericity of somatostatin expression in pretherapeutic [¹¹¹In]octreotide SPECT/CT might be a helpful parameter for prediction of lesion response to PRRT in patients with metastatic NEN.

Compliance with Ethical Standards. The Otto-von-Guericke-University Institutional Committee approved all procedures performed in this study in accordance with the ethical standards of the institutional research committee (ID number: RAD279; vote, 07/16) and with the 1964 Helsinki declaration and its later amendments or comparable ethical standards.

Conflict of Interest

The authors declare that they have no conflict of interest.

Informed Consent

Informed consent was obtained from all individual participants included in the study.

References

- Fani M, Maecke HR, Okarvi SM (2012) Radiolabeled peptides: valuable tools for the detection and treatment of cancer. *Theranostics* 2:481–501
- Pavel ME, Hainsworth JD, Baudin E et al (2011) Everolimus plus octreotide long-acting repeatable for the treatment of advanced neuroendocrine tumours associated with carcinoid syndrome (RADIANT-2): a randomised, placebo-controlled, phase 3 study. *Lancet* 378:2005–2012
- Kwekkeboom DJ, Teunissen JJ, Bakker WH et al (2005) Radiolabeled somatostatin analog [¹⁷⁷Lu-DOTA0,Tyr3]octreotate in patients with endocrine gastroenteropancreatic tumors. *J Clin Oncol* 23:2754–2762
- Strosberg J, Wolin E, Chasen B et al (2016) Progression-free survival, radiographic response, and preliminary overall survival results in patients with midgut neuroendocrine tumors treated with ¹⁷⁷Lu-Dotatate [abstract]. *J Clin Oncol* 34:4S
- Koerner M, Waser B, Reubi JC (2015) Does somatostatin or gastric inhibitory peptide receptor expression correlate with tumor grade and stage in gut neuroendocrine tumors. *Neuroendocrinology* 101:45–57
- Garin E, Le Jeune F, Devillers A et al (2009) Predictive value of 18F-FDG PET and somatostatin receptor scintigraphy in patients with metastatic endocrine tumors. *J Nucl Med* 50:858–864
- Hofman MS, Lau WFE, Hicks RJ (2015) Somatostatin receptor imaging with 68Ga DOTATATE PET/CT: clinical utility, normal patterns, pearls, and pitfalls in interpretation. *Radiographics* 35:500–516
- Kratochwil C, Stefanova M, Mavriopoulou E et al (2014) SUV of [⁶⁸Ga]DOTATOC-PET/CT predicts response probability of PRRT in neuroendocrine tumors. *Mol Imaging Biol* 17:313–318
- Li T-T, Qiu F, Qian ZR et al (2014) Classification, clinicopathologic features and treatment of gastric neuroendocrine tumors. *World J Gastroenterol* 20:118–125
- Apostolova I, Ego K, Steffen IG et al (2016) The asphericity of the metastatic tumour volume in NSCLC: correlation with histopathology and molecular markers. *Eur J Nucl Med Mol Imaging*. doi:10.1007/s00259-016-3452-z
- Davnall F, Yip CS, Ljungqvist G et al (2012) Assessment of tumor heterogeneity: an emerging imaging tool for clinical practice? *Insights Imaging* 3:573–589
- Yang Z, Tang LH, Klimstra DS (2011) Effect of tumor heterogeneity on the assessment of Ki67 labeling index in well-differentiated neuroendocrine tumors metastatic to the liver: implications for prognostic stratification. *Am J Surg Pathol* 35:853–860
- Lapa C, Werner RA, Schmid JS et al (2015) Prognostic value of positron emission tomography-assessed tumor heterogeneity in patients with thyroid cancer undergoing treatment with radiopeptide therapy. *Nucl Med Biol* 42:349–354
- Bakker WH, Albert R, Bruns C et al (1991) [¹¹¹In-DTPA-D-PHE1]-octreotide, a potential radiopharmaceutical for imaging of somatostatin receptor-positive tumors: synthesis, radiolabeling and in vitro validation. *Life Sci* 49:1583–1591
- Ezziddin S, Logvinski T, Yong-Hing C et al (2006) Factors predicting tracer uptake in somatostatin receptor and MIBG scintigraphy of metastatic gastroenteropancreatic neuroendocrine tumors. *J Nucl Med* 47:223–233
- Ramage JK, Ahmed A, Ardill J et al (2012) Guidelines for the management of gastroenteropancreatic neuroendocrine (including carcinoid) tumours (NETs). *Gut* 61:6–32
- Apostolova I, Steffen IG, Wedel F et al (2014) Asphericity of pretherapeutic tumour FDG uptake provides independent prognostic value in head-and-neck cancer. *Eur Radiol* 24:2077–2087
- Apostolova I, Steffen IG, Rogasch J et al (2014) Predictive value of asphericity of pretherapeutic FDG uptake in NSCLC. *J Nucl Med* 55:125–125
- Apostolova I, Rogasch J, Buchert R et al (2014) Quantitative assessment of the asphericity of pretherapeutic FDG uptake as an independent predictor of outcome in NSCLC. *BMC Cancer*. doi:10.1186/1471-2407-14-896
- Hofheinz F, Lougovski A, Zöphel K et al (2015) Increased evidence for the prognostic value of primary tumor asphericity in pretherapeutic FDG PET for risk stratification in patients with head and neck cancer. *Eur J Nucl Med Mol Imaging* 42:429–437
- Warner JA, Gladkiss LG, Geruschke T et al (2010) Tracing wear debris pathways via ion-implanted indium-111. *Wear* 268:1257–1265
- Kwekkeboom DJ, Krenning EP, Scheidhauer K et al (2009) ENETS consensus guidelines for the standards of care in neuroendocrine tumors: somatostatin receptor imaging with ¹¹¹In-pentetreotide. *Neuroendocrinology* 90:184–189
- Frilling A, Sotiropoulos GC, Radtke A et al (2010) The impact of 68Ga-DOTATOC positron emission tomography/computed tomography on the multimodal management of patients with neuroendocrine tumors. *Ann Surg* 252:850–856
- Pech M, Mohnike K, Wieners G et al (2008) Radiotherapy of liver metastases. *Strahlenther Onkol* 184:256–261
- Eisenhauer EA, Therasse P, Bogaerts J et al (2009) New response evaluation criteria in solid tumours: revised RECIST guideline (version 1.1). *Eur J Cancer* 45:228–247
- Hofheinz F, Langner J, Petr J et al (2013) An automatic method for accurate volume delineation of heterogeneous tumors in PET. *Med Phys* 40:082503
- Hofheinz F, Pöttsch C, Oehme L et al (2012) Automatic volume delineation in oncological PET. Evaluation of a dedicated software tool and comparison with manual delineation in clinical data sets. *Nucl Med* 51:9–16
- Maxwell JE, Howe JR (2015) Imaging in neuroendocrine tumors: an update for the clinician. *International Journal of Endocrine Oncology* 2:159–168
- Reubi JC, Schaer JC, Waser B et al (2000) Affinity profiles for human somatostatin receptor subtypes SST1–SST5 of somatostatin radiotracers selected for scintigraphic and radiotherapeutic use. *Eur J Nucl Med* 27:273–282
- Limouris GS, Poulantzas V, Trompoukis N et al (2015) Comparison of ¹¹¹In-[DTPA0] octreotide versus non carrier added ¹⁷⁷Lu-[DOTA0, Tyr3]-octreotate efficacy in patients with GEP-NET treated intra-arterially for liver metastases. *Clin Nucl Med* 41:194–200
- Klimstra DS, Modlin IR, Domenico C et al (2010) The pathologic classification of neuroendocrine tumors: a review of nomenclature, grading, and staging systems. *Pancreas* 39:707–712
- Srirajaskanthan R, Kayani I, Quigley AM et al (2010) The role of ⁶⁸Ga-DOTATATE PET in patients with neuroendocrine tumors and negative or equivocal findings on ¹¹¹In-DTPA-octreotide scintigraphy. *J Nucl Med* 51:875–882